Available online at www.sciencedirect.com

ScienceDirect

Ceramics International 40 (2014) 3579–3587

CERAMICS INTERNATIONAL

www.elsevier.com/locate/ceramint

Effect of Ho^{3+} doping on the electric, dielectric, ferromagnetic properties and T_C of $BiFeO_3$ ceramics

G.L Song[a,b], G.J. Ma[a], J. Su[a], T.X. Wang[a,b], H.Y. Yang[a,b], F.G. Chang[a,b,*]

[a]College of Physics and Information Engineering, Henan Normal University, Xinxiang 453007, China
[b]Henan Key Laboratory of Photovoltaic Materials, Xinxiang 453007, China

Received 19 August 2013; received in revised form 14 September 2013; accepted 14 September 2013
Available online 21 September 2013

Abstract

Multiferroic $Bi_{1-x}Ho_xFeO_3$ ($x=0$, 0.05, 0.1, 0.15, 0.2) ceramics have been prepared by rapid liquid phase sintering method. The effect of Ho doping on the structure, electrical, dielectric, ferromagnetism properties and T_C of $BiFeO_3$ ceramics is studied. The result shows that all the peaks for $Bi_{1-x}Ho_xFeO_3$ samples can be indexed according to the crystal structure of pure $BiFeO_3$ by XRD. When $x=0.15$ and 0.2, the samples consist of two phases including rhombohedral and orthorhombic. Ho doping $BiFeO_3$ enhanced the electrical properties with lower leakage current density. This dielectric behavior of $Bi_{1-x}Ho_xFeO_3$ ceramics varies with content x and frequency, which might be understood in terms of oxygen vacancy, the displacement of Fe^{3+} ions and lattice phase transition. The magnetic moment of $Bi_{1-x}Ho_xFeO_3$ ceramics varies with temperature from 300 to 1000 K at 5 kOe. It shows that the T_N of $BiFeO_3$ changes slightly from 638 K to 632 K with Ho^{3+} doping. The magnetic Curie temperature of $Bi_{1-x}Ho_xFeO_3$ will reduce from 970 K to 890 K with increasing Ho^{3+} content, depending mainly on the Fe–O–Fe super-exchange and magnetic structure of relative stability. By measuring the magnetic hysteresis loops, all the samples exhibit weak ferromagnetic behavior under 890 K and paramagnetism above 890 K. It evidences that the ferromagnetic phase transition of $Bi_{1-x}Ho_xFeO_3$ samples occurs at 890 K.

Keywords: Multiferroic material; Ferromagnetic; Magnetic hysteresis loops; The magnetic Curie temperature

1. Introduction

In recent years, multiferroic material is a time honored research subject due to its potential applications for the future technology in information storage, sensors, and for exploring physical phenomena in the coupling mechanism between electronic and magnetic order parameters [1–4].

Among them, $BiFeO_3$ (BFO) with a distorted perovskite (ABO_3) structure becomes the most extensively studied multiferroic material because of its ferroelectric transition temperature ($T_C \sim 1100$ K) and anti-ferromagnetic Néel temperature ($T_N \sim 640$ K) well above the room temperature [2–5].

However, the high leakage current and weak macroscopic magnetism of $BiFeO_3$ are the main barrier to its practical applications. How to decrease current leakage and improve the magnetic properties without disturbing the ferroelectric properties is essential in device applications.

In order to overcome these problems, many attempts have been done recently, great efforts have been focused on ferroelectric property, ferromagnetism, magnetoelectric effect of the multiferroic material $BiFeO_3$ [5–14]. Theoretically, Neaton et al. investigated spontaneous electric polarization of $BiFeO_3$ using local spin-density approximation (LSDA) and LSDA+U methods. It is found that the spontaneous electric polarization is around 90–100 μC/cm^2 [5]. Kornev et al. investigated high temperature magnetic of $BiFeO_3$ using Monte Carlo (MC) simulations methods. It is found that the aniferromagnetic phase transition T_N of $BiFeO_3$ is around 625–645 K and ferromagnetic phase transition T_C of $BFeO_3$ is around 750 K [6,7].

*Corresponding author at: College of Physics and Information Engineering, Henan Normal University, Xinxiang 453007, China. Tel.: +86 373 3326331; fax: +86 373 3326832.
E-mail addresses: chfg@htu.cn, guilinyichen@163.com (F.G. Chang).

0272-8842/$ - see front matter © 2013 Published by Elsevier Ltd and Techna Group S.r.l.
http://dx.doi.org/10.1016/j.ceramint.2013.09.070

Experimentally, the magnetic properties in $BiFeO_3$ were further modified by substitution of either A sites (Bi) with rare earth (La, Eu, Ho, Sm, Gd) [8–13] or B sites (Fe) with transition-metal (Co, Mn, Ni, Cr) [14,15] or A–B sites with rare earth and transition-metal leads to improved ferroelectric and ferromagnetic properties [16–18]. Singh et al. reported Bi-site substitution by lanthanide atoms such as La^{3+} is effective in controlling the volatility of Bi^{3+} by suppressing the formation of oxygen vacancies as well as one effective method for reducing the leakage current density [8–10]. Yao et al. reported that activation energy of 0.7 eV for the conduction process was found to be irrespective of the Sm^{3+} doping, the Néel temperature (T_N) decreased with increasing Sm^{3+} doping [11,12]. Pradhan et al. reported that Ho substitution at Bi site is likely to suppress the spiral spin modulation and increase the canting angle, which favors enhanced multiferroic properties [12]. Zhang et al. reported $Bi_{0.85}La_{0.1}Ho_{0.05}FeO_3$ multiferroic ceramics exhibited obvious ferroelectric loop with a remnant polarization of 11.2 μC/cm^2, weak ferromagnetism with the remnant magnetization of 0.179 emu/g and the dielectric constant decreases with increasing applied magnetic fields, the coupling coefficient reaches −1.04% at 10 kOe [13]. Naganuma reported that both the ferroelectric and magnetic properties of $BiFeO_3$ films can be enhanced by Co^{3+} doping, with the remnant polarization of $BiFeO_3$ films increased from 49 to 72 μC/cm^2 by addition of 3% Co^{3+} doping, the saturation magnetization drastically enhanced by doping Co^{3+} up to 12% [14,15]. Yang et al. observed saturated ferroelectric hysteresis characteristics in La–Co co-doped BFO thin films. However, they did not measure the temperature dependent magnetic moment variation of $Bi_{1-x}La_xFe_{1-y}Co_yO_3$ [16–18].

It is well known that the $HoFeO_3$ is a magnetic material having spontaneous magnetization and it has good dielectric properties [19]. A characteristic feature of $HoFeO_3$ is the presence of two magnetic subsystems: base on the rare-earth and the iron ions respectively. As far as we known, mechanism of Ho substitution at Bi site in $BiFeO_3$ system is still not clear and the results of reported is not inconsistent.

In this work, polycrystalline $Bi_{1-x}Ho_xFeO_3$ ($x=0$, 0.05, 0.1, 0.15, 0.2) ceramics specimen have been prepared with rapid liquid phase sintering method. Particularly, we focus on the dielectric, magnetic and high temperature magnetic phase transition properties of $Bi_{1-x}Ho_xFeO_3$ compound in order to study between 4*f* subshell of Ho and 3*d* subshell of Fe magnetic interaction mechanism. It is expected that Ho^{3+} doping could solve the high leakage current and weak macroscopic magnetism of $BiFeO_3$.

2. Experiment

The $Bi_{1-x}Ho_xFeO_3$ ($x=0$, 0.05, 0.1, 0.15, 0.2) ceramics were prepared by rapid liquid phase sintering method. The materials of Bi_2O_3, Fe_2O_3 and Ho_2O_3 (purity ≥ 99.99%) were carefully weighted in stoichiometric proportion and thoroughly mixed in an agate jar ball-milling machine for about 24 h using high purity isopropyl alcohol as a medium. The mixture was dried and pressed into disks with diameter of about 13 mm and thickness 1 mm. Then, the disks were sintered at 880 °C for 450 s in air and subsequently quenched to room temperature naturally. All samples were carefully polished before the addiction of Ag electrodes on both surfaces to form metal–insulator–metal capacitors. Details of sample preparation processes can be found in Ref [20].

The crystalline structure of the $Bi_{1-x}Ho_xFeO_3$ samples was characterized by x-ray diffraction (XRD) using a diffractometer with Cu Ka1 radiation. The unit cell parameters of the $Bi_{1-x}Ho_xFeO_3$ samples obtained by Rietveld refinement of the XRD patterns. The dielectric property measurement was performed by a precision impedance analyzer (HP4294A) with the frequency ranging from 40 Hz to 110 MHz. The magnetic property of $Bi_{1-x}Ho_xFeO_3$ was measured by a vibrating sample magnetometer integrated in a physical property measurement system (Versa Lab, Quantum Design).

3. Results and discussion

Fig. 1 presents the x-ray diffraction (XRD) patterns of $Bi_{1-x}Ho_xFeO_3$ ceramic samples ($x=0$, 0.05, 0.1, 0.15, 0.2). It

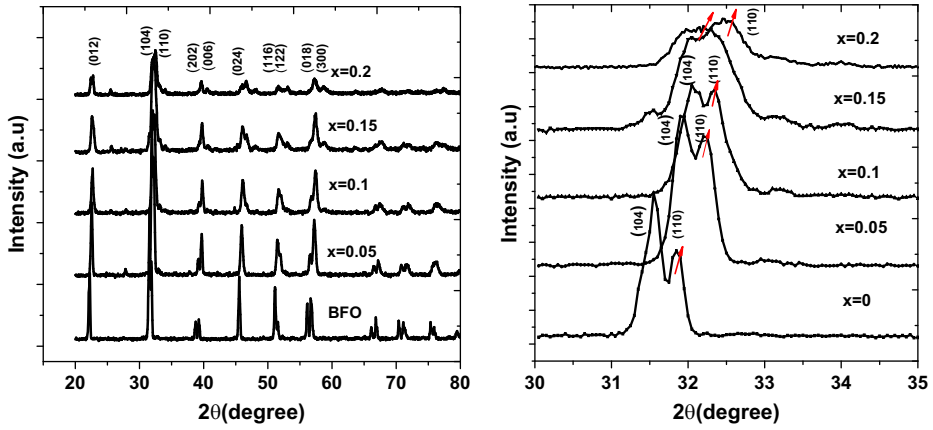

Fig. 1. Fig. 1 X-ray diffraction (XRD) patterns of $Bi_{1-x}Ho_xFeO_3$ samples (a) XRD patterns of $Bi_{1-x}Ho_xFeO_3$ and (b) XRD patterns $Bi_{1-x}Ho_xFeO_3$ in the range of 2θ from 30° to 34°).

can be seen that the ceramics show single-phase materials crystallizing. The XRD patterns show polycrystalline behavior with good crystallinity. We have not found the impurity phases ($Bi_2Fe_4O_9$ and $Bi_{46}Fe_2O_{72}$) were reported in literature.

Careful analyzation of XRD pattern in Fig. 1 revealed that the characteristic diffraction peaks of samples became gradually wider and shift to higher angles with Ho^{3+} doping. From these characters, we can draw the following conclusions:

(i) $Bi_{1-x}Ho_xFeO_3$ samples prepared by rapid liquid phase sintering method are better than that by solid state reaction method. According to Bi_2O_3–Fe_2O_3 phase diagram, it mentions the eutectic temperature at 785 °C, $BiFeO_3$ sample is an incongruently melting compound [18,21]. Quenching the sample is helpful in keeping the metastable $BiFeO_3$ single-phase at room temperature. The liquid phase accelerates the synthesizing reaction and probably prevents the formation of the second phase (for example: $Bi_2Fe_4O_9$). Hence, we have not found the impurity phases ($Bi_2Fe_4O_9$ and $Bi_{46}Fe_2O_{72}$) in our samples as reported in literature [18].

(ii) It can be seen from Fig. 1(b) that there is a slight move of the main peaks to a bigger angle 2θ with the increase of Ho. This shift in the diffraction angle might be ascribed to the unit cell contraction or the decrease in lattice constants because the ion radius of Ho^{3+} ($R_{Ho3+}=0.0905$ nm) is smaller than that of Bi^{3+} ion ($R_{Bi3+}=0.103$ nm) [8–13,17].

In order to further analyze such transformation, the measured XRD patterns of $Bi_{1-x}Ho_xFeO_3$ samples were analyzed with Rietveld refinement program. The best fits to the measured data are observed using rhombohedral lattice type with R3c space group for $x \leq 0.10$ samples (JCPDS20-10169) and with orthorhombic lattice type with Pnma space group for $x \geq 0.15$ samples (JCPDS14-0181) [8]. Based on our analysis, details of the *hkl* index with refined unit cell parameters are shown in Table 1. It is noted from Table 1 that with the increasing concentration of Ho in $BiFeO_3$, i. e. for $x=0$–0.10, the cell parameters (a_r and c_r) of $Bi_{1-x}Ho_xFeO_3$ are marginally reduced, as a result of unit cell volume contraction.

(iii) Fig. 1(b) reveals that the (104) and (110) peaks of $BiFeO_3$ in the 2θ ranges of 31–33° merged partially to form a broadened peak (110) at $x \geq 0.15$. Such a behavior indicates the propensity of the structure undergoing phase transformation from a rhombohedral to an orthorhombic structure with Ho substitution [12,13,22]. $Bi_{1-x}Ho_xFeO_3$ (x=0.15, 0.2) has orthorhombic symmetry with lattice parameters a=0.554673 nm, c=0.6893 nm for x=0.15 and a=0. 5564 nm, c=0. 6883 nm for x=0.2. The similar behavior has also been reported in Gd-doped $BiFeO_3$, which corresponds to a lattice distortion, phase transformation from a rhombohedral to an orthorhombic structure [8,22,24]. It can be inferred that the crystal structure of $BiFeO_3$ sample doped with proper concentration of elements can effectively modulate the structure of $BiFeO_3$ [25,26].

Fig. 2 exhibits the plots of the leakage current density–applied electric field (J–E) behavior of the $Bi_{1-x}Ho_xFeO_3$ ceramics. The current density curves of all the $Bi_{1-x}Ho_xFeO_3$ measured in this study are symmetrical. Therefore, the leakage behavior of all the samples is discussed only in a positively applied electric field. The leakage current increases rapidly with the applied electric field increasing from the Fig. 2 (semilog J–E plot). It can be seen that the leakage current of $Bi_{1-x}Ho_x$ FeO_3 gradually decreases with more Ho content doping under the same electric field. The leakage current densities of $Bi_{1-x}Ho_xFeO_3$ (x=0, 0.05, 0.1, 0.15, 0.2) were 1.94×10^{-3}, 2.35×10^{-3}, 2.22×10^{-3}, 9.57×10^{-6}, 6.29×10^{-6} A/cm^2 at electric field of 4000 V/cm, respectively.

Pure $BiFeO_3$ samples shows higher leakage current densities compared with Ho-doped $BiFeO_3$ compound. It might be due to the appearance of charged defects governed by Fe^{2+} ions, oxygen vacancies V_O and/or bismuth vacancies V_{Bi} in $BiFeO_3$

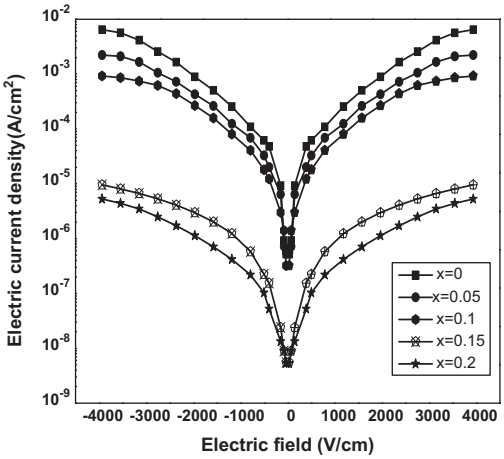

Fig. 2. The electric current density (J) vs electric field (E) curves for $Bi_{1-x}Ho_xFeO_3$ samples.

Table 1
The structural parameters (a, c, V), t (tolerance factor), M_s, M_r, T_N and T_C parameters for $Bi_{1-x}Ho_xO_3$ceramics.

Samples	$a=b$ (Å)	c (Å)	V (Å^3)	t	M_r (emu/g)	M_s (emu/g)	T_N (K)	T_C (K)
BFO	5.601	13.921	378.26	0.9052	0.0024	0.20195	638	970
BFO-Ho5%	5.579	13.812	372.35	0.9020	0.0075	0.49691	635	890
BFO-Ho10%	5.558	13.771	368.37	0.8988	0.0054	0.93133	632	890
BFO-Ho15%	5.547	6.894	183.68	0.8956	0.1146	1.05938	632	890
BFO-Ho20%	5.564	6.883	184.52	0.8923	0.1167	1.28064	632	890

sample [27,28]. According to the following reaction mechanisms [17,29]:

$$2Bi^{3+} + 3O^{2-} \rightarrow Bi_2O_3\uparrow + 2V^{3-}{}_{Bi} + 3V^{2+}{}_{O} \quad (1)$$

$$2Fe^{3+} + O^{2-} \rightarrow 2Fe^{2+} + 0.5O_2\uparrow + 2V_O{}^{2+} \quad (2)$$

Importantly, the presence of V_O^{2+} vacancy and V_{Bi}^{3-} as stated in Eqs. (1) and (2) has the predominant effect on the reduction of the electrical resistivity of the bulk samples, giving rise to high leakage currents in the samples [27–29]. With the Ho doping, the better leakage characteristics of $Bi_{1-x}Ho_xFeO_3$ samples are obtained. The leakage current of $Bi_{1-x}Ho_xFeO_3$ (x=0.05, 0.1) specimen is slightly lower than that of $BiFeO_3$. However, the J of $Bi_{1-x}Ho_xFeO_3$ (x=0.15, 0.2) is three orders of magnitude lower than that of $BiFeO_3$ under 4000 V/cm in Fig. 2. It is inferred that the origin of reduced leakage current in the $Bi_{1-x}Ho_xFeO_3$ is synergetic effect of "suppression of oxygen vacancies V_O and/or bismuth vacancies V_{Bi}" leading to reduce Fe^{2+} ions [17,29]. It shows that Ho doping $BiFeO_3$ enhanced the electrical properties with lower leakage current density. The result is consistent with the results reported by Singh et al. [8–10,25,28].

Fig. 3 shows the dielectric constant (ε_r) of $Bi_{1-x}Ho_xFeO_3$ (x=0, 0.05, 0.1, 0.15, 0.2) samples as a function of frequency (100 Hz–10 MHz) at room temperature. It is striking to see that the dielectric constant increases dramatically with small amount of Ho substitution (x=0.05, 0.10). For example, the dielectric constant measured at 1 kHz reaches a maximum value of ε_r=2899.3 when x=0.1, three times as big as that of pure $BiFeO_3$ (ε_r=967.8) inset Fig. 3. The obtained value of dielectric constant at room temperature for $BiFeO_3$ composition is comparable with the other reported values [4,24]. However, further increasing the Ho content (x=0.15, 0.2), the value of the dielectric constant is back to the level of pure $BiFeO_3$. To further investigate the effect of Ho Substitution on the dielectric property of these samples, the dielectric constant of $Bi_{1-x}Ho_xFeO_3$ are re-plotted in Fig. 3 inset as a function of Ho concentration x at 1 kHz, 10 kHz, 100 kHz respectively.

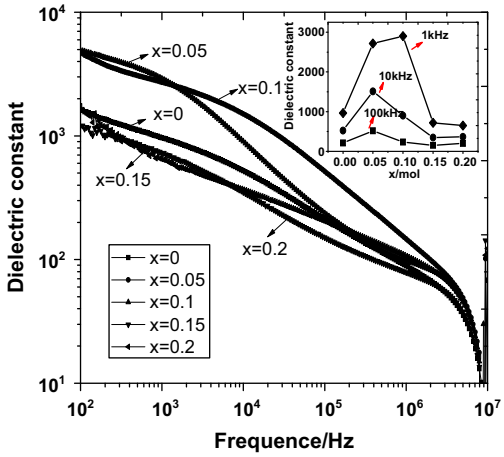

Fig. 3. Dielectric constant (ε_r) vs frequency curves for all samples (inset on the top right corner shows the dielectric constant of $Bi_{1-x}Ho_xFeO_3$ as a function of Ho concentration x at 1 kHz, 10 kHz, 100 kHz respectively).

This dielectric behavior of $Bi_{1-x}Ho_xFeO_3$ ceramics varies with content x and frequency, which might be understood in terms of oxygen vacancy, the displacement of Fe^{3+} ions and lattice phase transition.

It is well known that $BiFeO_3$ is distorted triangle perovskite structure belonging to R3c space group, whose spontaneous polarization is mainly ascribed to the relative displacement of Fe^{3+} ion against Fe–O octahedron [2,5,6,9,17,23,25]. Doping or substitution always leads to contraction of unit cell in isotropic ferroelectric ceramics. Because the radius of Ho^{3+} (R_{Ho3+}=0.0905 nm) is less than that of Bi^{3+} (R_{Bi3+}=0.103 nm), Ho doping causes distortion of oxygen octahedral, and enhances the dipole movement of Fe^{3+} along the (111) direction, resulting in increase in the dielectric constant of doped samples.

Compared with Bi^{3+} ion (R_{Bi3+}=1.03 Å), Ho^{3+} ion (R_{Ho3+}= 0.905 Å) possesses a much smaller radius. As the smaller, less polarizable Ho^{3+} substitutes for Bi^{3+} ions, the tolerance factor (t) decrease [8]

$$t = \frac{(R_A + R_O)}{\sqrt{2}(R_B + R_O)} \quad (3)$$

where R_A, R_B, and R_O are the ionic radii of the A, B, and O sites. The tolerance factor of $Bi_{1-x}Ho_x$ FeO_3 (x=0.05, 0.1, 0.15, 0.2) are shown in Table 1. When the tolerance factor is smaller than unity, the Fe–O bonds are under compression and the Bi^{3+}/Ho^{3+}–O bonds are under tension. The oxygen octahedra then tend to rotate cooperatively to alleviate the lattice stress and the relative rotation angle of the two oxygen octahedra around the polarization [111] axis in the R3c unit cell for the samples increases with substitution of Ho for Bi in $BiFeO_3$ [8].

There are always some oxygen vacancies in pure $BiFeO_3$. It can be seen from Fig. 2 that the leakage current density of $BiFeO_3$ is highest in all samples at application electric field, indicating relatively high conductivity and small dielectric constant [29,30]. Substitution of small amount of Ho^{3+} for Bi^{3+} will reduce the number of oxygen vacancies and Fe^{2+}. It will decrease the leakage current density of the $BiFeO_3$ ceramics and increase the dielectric constant of $BiFeO_3$.

With further increasing in the Ho content (x=0.15, 0.2), the value of the dielectric constant will be reduced to pure $BiFeO_3$. The dielectric properties of $Bi_{1-x}Ho_xFeO_3$ (x=0.15, 0.2) ceramics can be attributed to the modified structure, because dielectric properties are highly dependent on the sample structure and are easily modulated when they are near phase transformation boundary [16]. From Table 1, we found that the $Bi_{1-x}Ho_xFeO_3$ (x=0.15, 0.2) samples corresponds to lattice phase transformation from a rhombohedral (R3c space group) to an orthorhombic structure (Pnma space group). This space group (Pnma) is centrosymmetric and detrimental to ferroelectric as well as multiferroic properties leading to decrease of dielectric constant [12].

Fig. 4 shows the frequency dependence of dielectric loss in $Bi_{1-x}Ho_xFeO_3$ ceramics. The dielectric loss of $Bi_{1-x}Ho_xFeO_3$ increases with frequency in accordance with Debye relaxation theory. The dielectric loss of $BiFeO_3$ decreases with frequency increasing with sign of loss peak at 80 kHz, which is consistent

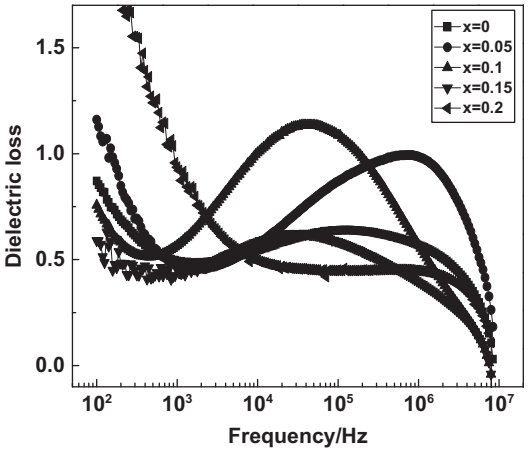

Fig. 4. Dielectric loss (tan δ) vs frequency curves for all samples.

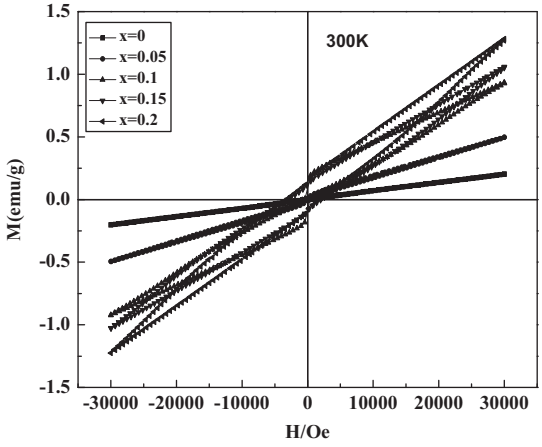

Fig. 5. Magnetization vs magnetic field curves for samples $Bi_{1-x}Ho_xFeO_3$ at RT.

with a combined response of orientational relaxation of dipoles and the conduction of charge carriers. The similar results have been reported by Palkar and Ueda [31,32]. However, Palkar et al. only reported dielectric loss that showed a decrease with frequency, a dip appeared just above 105 kHz and then rising again [31]. Ueda et al. also reported a similar dip in thin films of $BiFeO_3$–$BaTiO_3$ solid solution [32].

With increasing Ho content x, the loss peaks shift toward high frequency at 110 kHz, 1 MHz, respectively. By comparing the dielectric loss (Fig. 4) with the leakage current presented (Fig. 2), it can be concluded that the dielectric loss is dominated by the conductivity of the material. The contribution from other mechanisms such as orientational polarization of dipoles is relatively small. This is particularly true for the dielectric loss of low frequency such as at 1 kHz, which follows a similar trend as the dc conductivity i.e. the inverse of the current density. The dielectric properties and the current density of $Bi_{1-x}Ho_xFeO_3$ are related. It suggests that the leakage current plays an important role in the material.

The dielectric loss of $Bi_{1-x}Ho_xFeO_3$ samples behaves in a complicated way with a few debye peaks, which are lower than that of pure $BiFeO_3$. Relaxation time dispersion theory indicates that the relaxation time of most dielectric material disperses in the relaxation process, and the material have energy absorption characteristics in a number of frequencies, so a few Debye peaks are present in the curves at Fig. 4.

Fig. 5 shows the magnetic hysteresis loops of $Bi_{1-x}Ho_xFeO_3$ ceramics with an applied field up to 3 T at room temperature. M–H of all samples illustrate a typical weak ferromagnetic ordering. For pure $BiFeO_3$, M–H curves exhibit roughly linear field dependence of magnetization at room temperature. But a nonlinear behavior of the M–H curve can be seen with enlarged scales as shown in Fig. 6 inset. The remnant magnetization of pure $BiFeO_3$ (M_r) is 0.0024 emu/g, indicating that Pure $BiFeO_3$ ceramic is weakly ferromagnetic. The result agreed respectively with that reported by Du et al. [12,13,23–27].

The Ho^{3+} doping results in the appearance of weak and complete magnetic hysteresis loops at room temperature. The remnant magnetization values of $Bi_{1-x}Ho_xFeO_3$ for x=0, 0.05, 0.10, 0.15 and 0.2 are in the following order: 0.0024, 0.0075, 0.084, 0.1146, 0.1167 emu/g, namely, the M_r of $Bi_{1-x}Ho_xFeO_3$ is 3.1, 35, 47.75 and 48.6 times of that of $BiFeO_3$, respectively. The M_s, M_r, T_N and T_C parameters for $Bi_{1-x}Ho_xFeO_3$ ceramics are summarized in Table 1. Three possible explanations may account for weak ferromagnetism in $Bi_{1-x}Ho_xFeO_3$ samples.

i) $BiFeO_3$ exhibits weak ferromagnetism. For pure $BiFeO_3$ ceramic exhibits weak ferromagnetism, Xu et al. believed that it was due to the induced lattice distortion by the rapid sintering and fast cooling process [33]. The high field linear M–H relationship was commonly observed in bulk $BiFeO_3$ which was due to the anti-ferromagnetic arrangement of Fe^{3+} spins. However, oxygen vacancies of $BiFeO_3$ sample lead to the presence of Fe^{2+}. Fe^{3+}–O^{2-}–Fe^{2+} magnetic exchange should have important impact on the magnetic properties of these samples. Ionic radius of Fe^{2+} is almost 15% larger than that of Fe^{3+}, which can cause distortion in the crystal structure, resulting in titrations of the collinear spin arrangement in [111] planes and a non-zero net magnetic moment [34].

ii) The structure distortion. With Ho^{3+} doping, the unit cell contract or decrease in lattice constants of $BiFeO_3$, due to Ho^{3+} ionic radius (R_{Ho3+}=0.0905 nm) is smaller than that of Bi^{3+} (R_{Bi3+}=0.103 nm). In this work, Ho^{3+} substitution does not promote any major structural transformation in $Bi_{1-x}Ho_xFeO_3$ (x=0.05 and 0.1). The partial change (reduction) in unit cell volume with the increase of Ho^{3+} is observed in Fig. 1. The partial change may cause internal structural distortion relating to the change of inter atomic bond distances between Fe–O and Bi–O. Since the super-exchange interaction is sensitive to bond length and bond angle, the structure distortion can change Fe–O–Fe bond angle or suppress the spin spiral [18]. It releases potentially weak ferromagnetic order, which leads to enhancement of remnant magnetization in $BiFeO_3$ system by doping of Ho^{3+} [12,13,22]. However, when $x \geq 0.15$, the Ho^{3+} substitution results in structural phase transition,

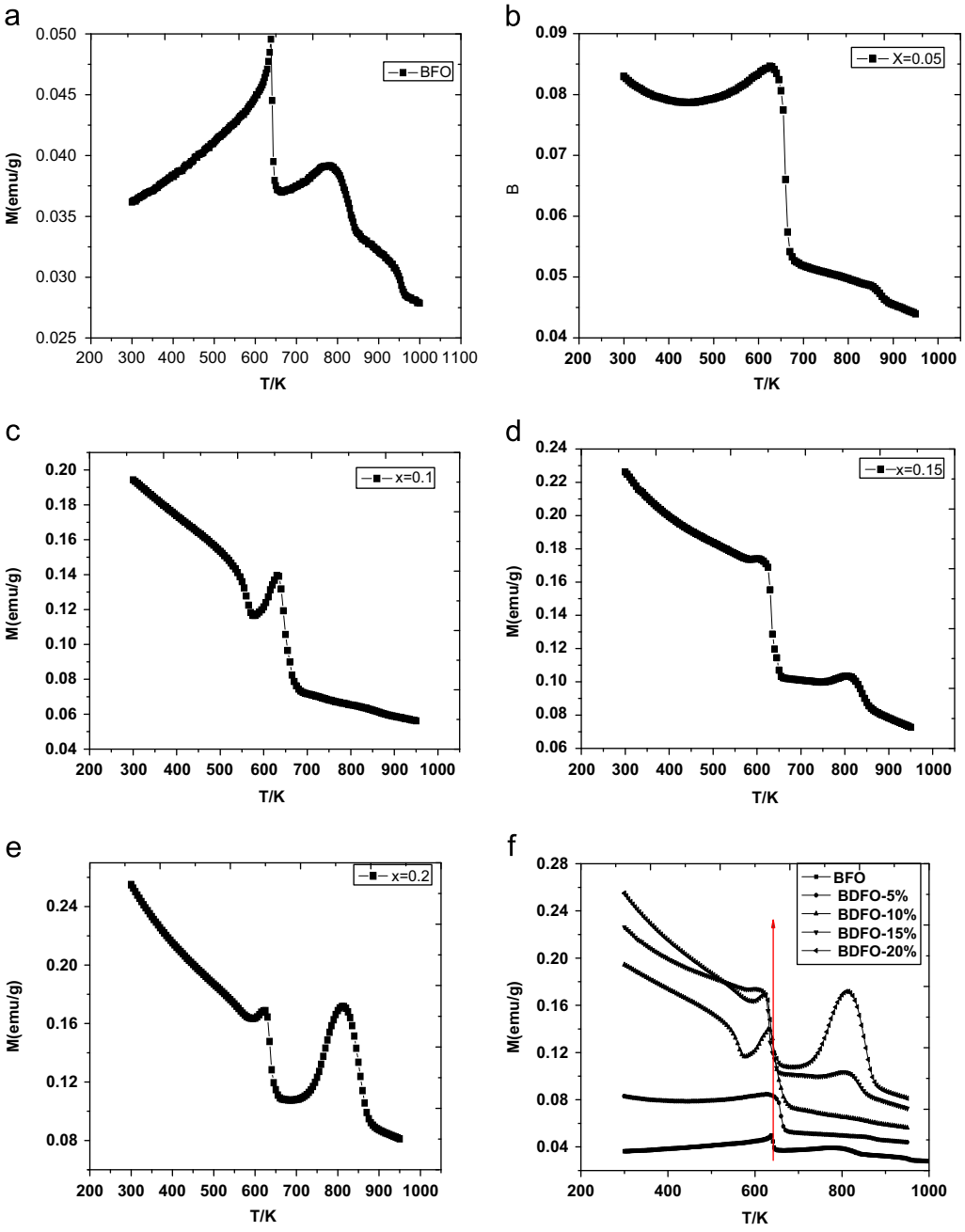

Fig. 6. Magnetization as a function of temperature for all samples from 300 K to 900 K in 5000 Oe field. (a) $BiFeO_3$, (b) $Bi_{0.95}Ho_{0.05}FeO_3$, (c)$Bi_{0.9}Ho_{0.1}FeO_3$, (d) $Bi_{0.85}Ho_{0.15}FeO_3$, (e)$Bi_{0.8}Ho_{0.2}FeO_3$ and (f) $Bi_{1-x}Ho_xFeO_3$.

wherein the spin cycloid might be destructed and homogeneous spin structure formed. It is observed that the latent magnetization locked within the cycloid might be released and the significant M_r value increased. However, Kang et al. found that addition of Ho drastically reduced the grain size to ~4–5 μm of $BiFeO_3$ and increased the density by ~6%. Changes in microstructure are expected to affect the dielectric and magnetic properties [35].

iii) The super exchange interaction. It can be found that the magnetization (M) of $Bi_{1-x}Ho_xFeO_3$ at 30 kOe is significantly larger than that of $BiFeO_3$ from Fig. 6. These behaviors should attribute to the contribution from the Ho^{3+} ions. There are three main interactions in rare earth–transition metal compounds, which is T–T (Fe^{3+}–Fe^{3+}), R–T (Ho^{3+}–Fe^{3+}) and R–R (Ho^{3+}–Ho^{3+}) exchange interaction. The T–T exchange interaction is the strongest, R–R exchange interaction is the weakest, and R–T exchange interaction is middle. Ho^{3+} is a magnetically active ion and has a large magnetic moment. When Bi^{3+} is substituted by an amount of Ho^{3+} ions, the exchange interaction between 4*f* subshell of Ho^{3+} and 3*d* subshell of Fe^{3+} is also possible to contribute to the enhancement of ferromagnetic properties of $Bi_{1-x}Ho_xFeO_3$ [22,26]. Kang et al. reported a similar contribution from the ferromagnetic

interaction of Fe^{3+} and Ho^{3+} is anticipated in Ho-doped samples [35]. These results are also in agreement with the results obtained in Gd, Sm and Dy rare earth doped $BiFeO_3$ systems [9–13,26].

Thermo-magnetic experiments of $B_{1-x}Ho_xFeO_3$ ceramics were performed for temperatures in the range of 300–950 K according to a FC sequence under a magnetic field H=0.5 T and the results are presented in Fig. 6(a–f). The variation of their magnetization against the temperature $M(T)$ shows indeed the presence of a temperature-dependent magnetic order, with magnetic moments (under the excitation field H=0.5 T) monotonously decreased with temperature. From Fig. 6, the FC process is characterized by two evident anomalies. The first one is approximately 640 K, showing the anti-ferromagnetic phase transition, which is in agreement with the reported Neel temperature (T_N=640 K) of $BiFeO_3$ samples [1–5]. It can be seen from the Fig. 6 that the T_N of $Bi_{1-x}Ho_xFeO_3$ is 632 K, which change a little with Ho^{3+} doping. The result is in agreement with that report by Yao et al. In the report the magnetic Néel temperature (T_N) decreased with increasing Sm^{3+} doping content [11].

Another anomaly of $BiFeO_3$ happens at 970 K, which is related to the magnetic Curie temperature of $BiFeO_3$ (T_C=970 K). However, the corresponding temperature of $B_{1-x}Ho_xFeO_3$ would be reduced from 970 K to 890 K with increasing x. At present, there are few reports about the high temperature magnetic measurements of rare earth doped $BiFeO_3$ and no one has mentioned this ferromagnetic phase transition at 890 K.

When Ho content is further increased from 0.05 to 0.2, the $Bi_{1-x}Ho_xFeO_3$ specimens exhibit a strong ferromagnetic behavior. The magnetic moments of $Bi_{1-x}Ho_xFeO_3$ decrease with temperature increasing. We found that the magnetic moments of $Bi_{1-x}Ho_xFeO_3$ changed from ferromagnetic to paramagnetic at 890 k. The phase transition temperature of doped samples moving to lower temperature from 970 K to 890 K demonstrate that Ho^{3+} doping decrease the Curie temperature (T_C) compared with that of pure $BiFeO_3$ samples.

Three possible explanations may account for the phase transition temperature of $Bi_{1-x}Ho_xFeO_3$ ceramics moving to lower temperature from 970 to 890 K.

First of all, with Ho^{3+} doping, the main diffraction peak between (104) and (110) of $BiFeO_3$ sample are overlapped (110) single peak gradually. Rhombohedra symmetry of $BiFeO_3$ has transformed to orthorhombic perovskite structure. The structure phase transition is one of the reasons which could lead to the Curie temperature of $BiFeO_3$ shifting from 970 K to 890 K.

Secondly, the enhancement of magnetization may also be attributed to the collapse of the spiral spin anti-ferromagnetic structure to form a new magnetic structure in $BiFeO_3$ in spite of the existence of magnetic coupling between the Fe–O–Fe and Ho–Fe super-exchange interaction with Ho^{3+} substituting Bi^{3+}. It could be a major reason that weak Fe–O–Fe super-exchange interaction and unstable magnetic structure of $Bi_{1-x}Ho_xFeO_3$ lead to the Curie temperature shifting toward low temperature of 890 K.

Thirdly, 4f of Ho^{3+} and 3d of Fe^{3+} form a weak exchange interaction (f–d exchange interaction) in $Bi_{1-x}Ho_xFeO_3$. But the f–d exchange interaction is relatively weak compared with d–d, a difference of one order of magnitude [36]. Therefore, the f–d exchange interaction did not affect the Curie temperature of $BiFeO_3$.

In conclusion, the Curie temperature of $Bi_{1-x}Ho_xFeO_3$ change depends mainly on the Fe–O–Fe super-exchange strength and relative stability of magnetic structure.

In order to verify the fact that the ferromagnetic phase transition of $Bi_{1-x}Ho_xFeO_3$ samples occurred at 970 K and 890 K, the magnetic hysteresis loops is measured for all samples with an applied magnetic field up to 3 T at 750 K, 900k and 1000 K, respectively. As it is shown in Fig. 7.

The magnetic hysteresis loops of $Bi_{1-x}Ho_xFeO_3$ samples exhibit linear at 900 K, indicating the paramagnetism. This is in consistent with Das' results [37]. Das reported that a large change in the magnetization was observed around 370 °C, which was close to the Neel temperature (T_N) of Ba-doped $BiFeO_3$, and another magnetic transition which exhibited linear M vs H behavior resembling the paramagnetism observed upon 600 °C [37,38]. Gheorghiu et al. reported that the magnetic Curie temperature of $BiFeO_3$ was ~860 K [38]. It evidenced that the ferromagnetic phase transition of $Bi_{1-x}Ho_xFeO_3$ samples occurred at 890 K in Fig. 7. It is different with our results of Ho^{3+} doped samples due to the lack of corresponding high temperature ferromagnetic transition experimental data in the literatures [16]. Here for the first time the transition temperature has been determined. Naturally, more experimental and theoretical works are needed to clarify the exact origin of this high temperature ferromagnetic transition.

To sun up the above arguments, we think that Ho-doping in $BiFeO_3$ ceramics is proved to be an effective way to modulate the structure and the magnetic properties. This is essential for practical applications.

4. Conclusion

Polycrystalline $Bi_{1-x}Ho_xFeO_3$ (x=0, 0.05, 0.1, 0.15, 0.2) samples were prepared in air by rapid liquid phase sintering method. The crystalline structure, ferromagnetism properties and the high ferromagnetic phase transition of $Bi_{1-x}Ho_xFeO_3$ ceramics have been studied in detail. The following conclusions have been reached:

[1] Main diffraction peak between (104) and (110) of $BiFeO_3$ samples gradually overlaped (110) to single peak with increasing x has been proved. It implies that rhombohedral symmetry has transformed to orthorhombic perovskite structure.

[2] The leakage current of $Bi_{1-x}Ho_x$ FeO_3 specimen is lower than that of $BiFeO_3$. The leakage current of $Bi_{1-x}Ho_x$ FeO_3 (x=0.15, 0.2) is three orders in magnitude lower than that of $BiFeO_3$ under 4000 V/cm.

[3] The dielectric constant of $BiFeO_3$ is enhanced with Ho^{3+} doping. The dielectric constant of $Bi_{0.9}Ho_{0.1}FeO_3$ measured at 1 kHz is about ten times larger than that of pure

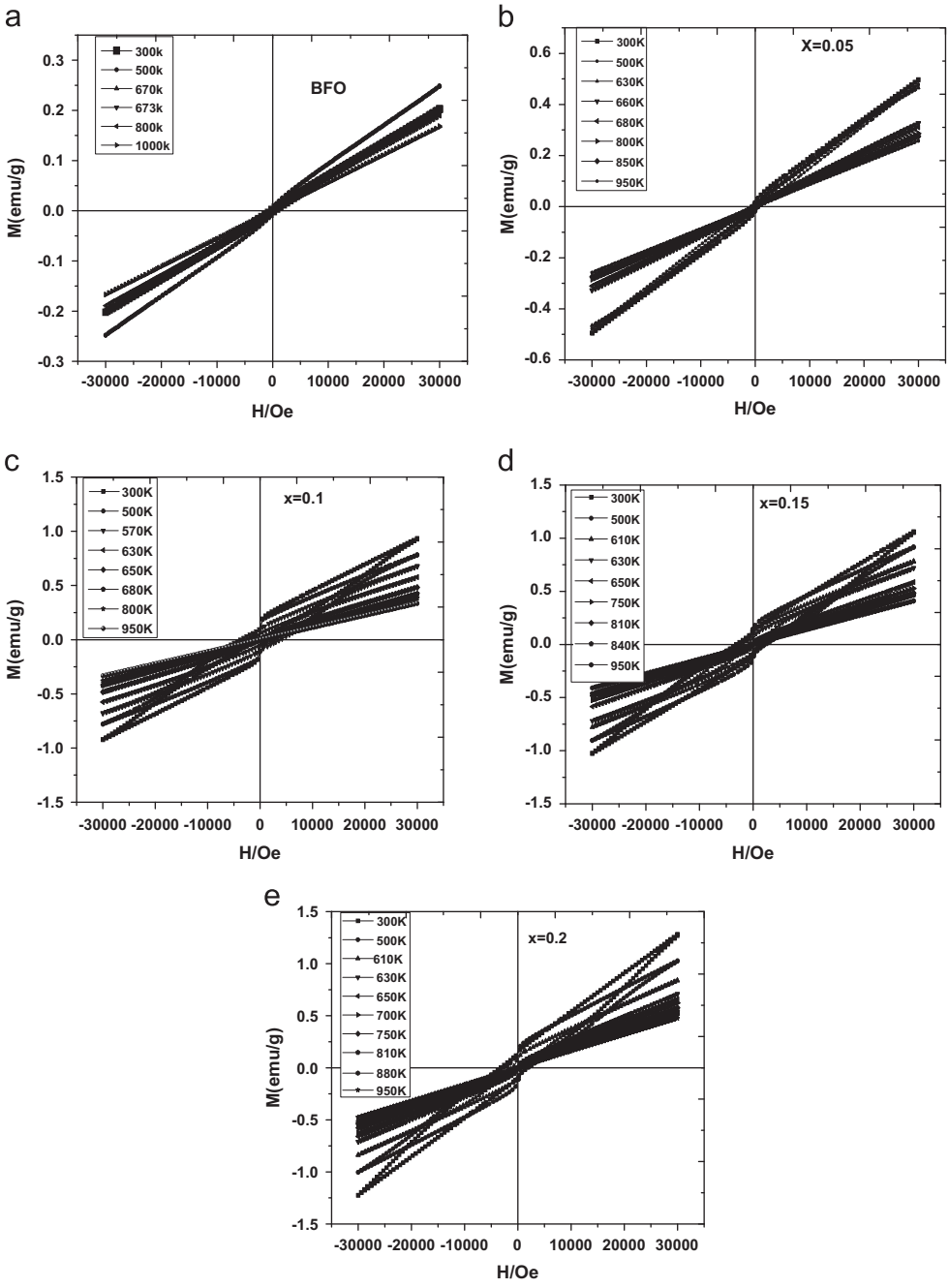

Fig. 7. Magnetization vs. magnetic field curves for samples $Bi_{1-x}Ho_xFeO_3$ at 600, 850, 900 and 950 K, respectively. (a) $BiFeO_3$, (b) $Bi_{0.95}Ho_{0.05}FeO_3$, (c)$Bi_{0.9}Ho_{0.1}FeO_3$, (d) $Bi_{0.85}Ho_{0.15}FeO_3$ and (e) $Bi_{0.8}Ho_{0.2}FeO_3$.

$BiFeO_3$. The dielectric loss of $Bi_{1-x}Ho_xFeO_3$ samples behaves in a complicated way with a few debye peaks, which are lower than that of pure $BiFeO_3$.

[4] All the samples of $Bi_{1-x}Ho_x$ FeO_3 ($x=0.05$, 0.1, 0.15, 0.2) exhibits weak ferromagnetic behavior below 890 K and paramagnetism above 890 K. It evidenced that the ferromagnetic phase transition of $Bi_{1-x}Ho_xFeO_3$ samples occurred at 890 K.

[5] The T_N of $BiFeO_3$ is 638 K, which does not change with Ho^{3+} doping. The magnetic Curie temperature of $BiFeO_3$ would be reduced from 970 K to 890 K with increasing x.

Acknowledgments

This work was supported by the National Natural Science Foundation of China (Project no: 60571063); the Basic and Advanced Technology Research Projects in Henan Province, China (Project no: 122300410203); Basic Research Program of Education Bureau of Henan Province, China (2011A140014).

References

[1] W. Eerenstein, N.D. Mathur, J.F. Scott, Multiferroic and magnetoelectric materials, Nature 442 (2006) 759–765.

[2] C.T. Nelson, P. Gao, J.R. Jokisaari, C. Heikes, C. Adamo, C.M. Folkman, C.B. Eom, D.G. Schlom, C.A. Melville, S.H. Baek, C.M. Folkman, B. Winchester, Y.J. Gu, Y.M. Liu, K. Zhang, E.G. Wang, J.Y. Li, L.Q. Chen, C.B. Eom, D.G. Schlom, X.Q. Pan, Domain dynamics during ferroelectric switching, Science 334 (2011) 968–971.
[3] M. Bibes, A. Barthélémy, Multiferroics: towards a magnetoelectric memory, Nature Materials 7 (2008) 425–426.
[4] C. Yang, C.Z. Liu, C.M. Wang, W.G. Zhang, J.S. Jiang, Magnetic and dielectric properties of alkaline earth Ca^{2+} and Ba^{2+} ions co-doped $BiFeO_3$ nanoparticles, Journal of Magnetism and Magnetic Materials 324 (2012) 1483–1487.
[5] J.B. Neaton, C. Ederer, U.V. Waghmare, N.A. Spaldin, K.M. Rabe, First-principles study of spontaneous polarizationin multiferroic $BiFeO_3$, Physical Review B 71 (2005) 014113–014121.
[6] A. Igor, S. Kornev, R. Lisenkov, B. Haumont, L. Bellaiche1, Finite-temperature properties of multiferroic $BiFeO_3$, Physical Review Letters 99 (2007) 227602–227605.
[7] H. Zhang, Y.J. Liu, L.H. Pan, Y. Zhang, First-principles study of Co doped $BiFeO_3$, Acta Physica Sinica 58 (2009) 7141–7146.
[8] X.Q. Zhang, Y. Sui, X.J. Wang, Y. Wang, Z. Wang, Effect of Eu substitution on the crystal structure and multiferroic properties of $BiFeO_3$, Journal of Alloys and Compounds 507 (2010) 157–161.
[9] K. Sen, K. Singh, Ashish Gautam, M. Singh, Dispersion studies of La substitution on dielectric and ferroelectric properties of multiferroic $BiFeO_3$ ceramic, Ceramics International 38 (2012) 243–249.
[10] V.A. Khomchenko, V.V. Shvartsman, P. Borisov, W. Kleemann, D.A. Kiselev, I.K. Bdikin, J.M. Vieira, A.L. Kholkin, Effect of Gd substitution on the crystal structure and multiferroic properties of $BiFeO_3$, Acta Materialia 57 (2009) 5137–5145.
[11] Y.B. Yao, W.C. Liu, C.L. Mak, Pyroelectric properties and electrical conductivity in samarium doped $BiFeO_3$ ceramics, Journal of Alloys and Compounds 527 (2012) 157–162.
[12] S.K. Pradhan, J. Das, P.P. Rout, V.R. Mohanta, S.K. Das, S. Samantray, D.R. Sahu, J.L. Huang, S. Verma, B.K. Roul, Effect of holmium substitution for the improvement of multiferroic properties of $BiFeO_3$, Journal of Physics and Chemistry of Solids 71 (2010) 1557–1564.
[13] X.Q. Zhang, Y. Sui, X.J. Wang, J.H. Mao, R.B. Zhu, Y. Wang, Z. Wang, Y.Q. Liu, W.F. Liu, Multiferroic and magnetoelectric properties of single-phase $Bi_{0.85}La_{0.1}Ho_{0.05}FeO_3$ ceramics, Journal of Alloys and Compounds 509 (2011) 5908–5912.
[14] H. Naganuma, N. Shimura, J. Miura, H. Shima, S. Yasui, S. Okamura, Enhancement of ferroelectric and magnetic properties in $BiFeO_3$ films by small amount of cobalt addition, Journal of Applied Physics 103 (2008) 07E314.
[15] E.-M. Choi, S. Patnaik, E. Weal, S.-L. Sahonta, H. Wang, Z. Bi, J. Xiong, M.G. Blamire, Q.X. Jia, J.L. MacManus-Driscoll, Strong room temperature magnetism in highly resistive strained thin films of $BiFe_{0.5}Mn_{0.5}O_3$, Applied Physics Letters 98 (2011) (012509-3).
[16] C.M. Raghavan, E.S. Kim, J.W. Kim, S.S. Kim, Structural and electrical properties of $(Bi_{0.9}Dy_{0.1})$ $(Fe_{0.975}TM_{0.025})$ $O_3 \pm \delta$ (TM=Ni^{2+}, Cr^{3+} and Ti^{4+}) thin films, Ceramics International 39 (2013) 6057–6062.
[17] G.L. Song, H.X. Zhang, T.X. Wang, H.G. Yang, F.G. Chang, Effect of Sm, Co co-doping on the dielectric and magnetoelectric properties of $BiFeO_3$ polycrystalline ceramics, Journal of Magnetism and Magnetic Materials 324 (2012) 2121–2126.
[18] A. Kumar, K.L. Yadav, Jyoti Rani, Low temperature step magnetization and magnetodielectric study in $Bi_{0.95}La_{0.05}Fe_{1-x}Zr_xO_3$ ceramics, Materials Chemistry and Physics 134 (2012) 430–434.
[19] D.G. Eorgiev, K.A. Krezhovt, V.V. Nietv, Weak antiferromagnetism in $YFeO_3$ and $HoFeO_3$, Solid State Communications 96 (1995) 535–537.
[20] Y.P. Wang, L. Zhou, M.F. Zhang, X.Y. Chen, J.M. Liu, Z.G. Liu, Room-temperature saturated ferroelectric polarization in $BiFeO_3$ ceramics synthesized by rapid liquid phase sintering, Applied Physics Letters 84 (2004) 1703–1704.
[21] J.D. Yu, N. Koshikawa, Y. Arai, S. Yoda, H. Saitou, Containerless solidification of oxide material using an electrostatic levitation furnace in microgravity, Journal of Crystal Growth 231 (2001) 568–576.
[22] Z.L. Hou, H.F. Zhou, L.B. Kong, H.B. Jin, X. Qi, M.S. Cao, Enhanced ferromagnetism and micro wave absorption properties of $BiFeO_3$ nanocrystals with Ho substitution, Materials Letters 84 (2012) 110–113.
[23] Z.X. Cheng, A.H. Li, X.L. Wang, S.X. Dou, K. Ozawa, H. Kimura, S. J. Zhang, T.R. Shrout, Structure, ferroelectric properties, and magnetic properties of the La-doped bismuth ferrite, Journal of Applied Physics 103 (2008) (07E507-3).
[24] J.B. Li, G.H. Rao, Y. Xiao, J.K. Liang, J. Luo, G.Y. Liu, Structural evolution and physical properties of $Bi_{1-x}Gd_xFeO_3$ ceramics, Acta Materialia 58 (2010) 3701–3708.
[25] K.G. Yang, Y.L. Zhang, S.H. Yang, B. Wang, Structural, electrical, and magnetic properties of multiferroic $Bi_{1-x}La_xFe_{1-y}Co_yO_3$ thin films, Journal of Applied Physics 107 (2010) (124109-5).
[26] G.L. Song, Y.P. Luo, J. Su, X.H. Zhou, F.G. Chang, Effects of Dy and Co co-substitution on the magnetic properties and TC of $BiFeO_3$ ceramics, Acta Physica Sinica 62 (2013) 097502–097508.
[27] Y. Du, Z.X. Cheng, S.X. Dou, Mahboobeh Shahbazi, X.L. Wang, Enhancement of magnetization and dielectric properties of chromium-doped $BiFeO_3$ with tunable morphologies, Thin Solid Films 518 (2010) 5–8.
[28] S. Kazhugasalamoorthy, P. Jegatheesan, R. Mohandoss, N.V. Giridharan, B. Karthikeyan, R. Justin Joseyphus, S. Dhanuskodi, Investigations on the properties of pure and rare earth modified bismuth ferrite ceramics, Journal of Alloys and Compounds 493 (2010) 569–572.
[29] G.L. Yuan, Siu Wing Ora, Multiferroicity in polarized single-phase $Bi_{0.875}Sm_{0.125}FeO_3$ ceramics, Journal of Applied Physics 100 (2006) 024109.
[30] V.R. Palkar, J. John, R. Pinto, Observation of saturated polarization and dielectric anomaly in magnetoelectric $BiFeO_3$ thin films, Applied Physics Letters 80 (2002) 1628–1630.
[31] M.M. Kumar, V.R. Palkar, K. Srinivas, S.V. Suryanarayana, Ferroelectricity in a pure $BiFeO_3$ ceramics, Applied Physics Letters 76 (2000) 2764–2766.
[32] K. Ueda, H. Tabat, T. Kawai, Coexistence of ferroelectricity and ferromagnetism in $BiFeO_3$–$BaTiO_3$ thin films at room temperature, Applied Physics Letters 75 (1999) (555-4).
[33] X.H. Zheng, Q.Y. Xu, Z. Wen, X.Z. Lang, D. Wu, T. Qiu, M.X. Xu, The magnetic properties of La doped and codoped $BiFeO_3$, Journal of Alloys and Compounds 499 (2010) 108–112.
[34] Y.-K. Jun, S.-H. Hong, Dielectric and magnetic properties in Co-and Nb-substituted $BiFeO_3$ ceramics, Solid State Communications 144 (2007) 329–333.
[35] Nari Jeon, Dibyaranjan Rout, Ill Won Kim, L. Suk-Joong, Kang, Enhanced multiferroic properties of single-phase $BiFeO_3$ bulk ceramics by Ho doping, Applied Physics Letters 98 (2011) 072901–072903.
[36] J.J.M. Franse, F.R. de Boer, P.H. Frings, R. Gersdorf, A. Menovsky, F. A. Muller, R.J. Radwanski, S. Sinnema, Magnetic transitions in single-crystal Ho_2Co_{17} studied in high magnetic fields, Physical Review B 31 (1985) (4346-4).
[37] R. Das, K. Mandal, Magnetic, ferroelectric and magnetoelectric properties of Ba-doped $BiFeO_3$, Journal of Magnetism and Magnetic Materials 324 (2012) 1913–1918.
[38] F.P. Gheorghiu, A. Ianculescu, P. Postolache, N. Lupu, M. Dobromira, D. Luca, L. Mitoseriu, Preparation and properties of $(1-x)BiFeO_3$–$xBaTiO_3$ multiferroic ceramics, Journal of Alloys and Compounds 506 (2010) 862–867.